Available online at www.sciencedirect.com
SCIENCE DIRECT
Journal of Catalysis 236 (2005) 55–61
JOURNAL OF CATALYSIS
www.elsevier.com/locate/jcat

Kinetics and mechanism of cyclohexane oxidation catalyzed by supramolecular manganese(III) porphyrins

Genebaldo S. Nunes, Ildemar Mayer, Henrique E. Toma, Koiti Araki *

Department of Fundamental Chemistry, Institute of Chemistry, University of São Paulo, USP, Caixa Postal 26077, São Paulo SP 05513-970, Brazil

Received 25 July 2005; revised 26 August 2005; accepted 2 September 2005

Available online 13 October 2005

Abstract

We report the kinetics of cyclohexane oxidation with iodosylbenzene, catalyzed by two supramolecular manganese(III) porphyrin isomers, containing four $[Ru(bpy)_2Cl]^+$ complexes attached to the pyridyl groups of *meso*-tetra(3-pyridyl)porphynatemanganese(III) or *meso*-tetra(4-pyridyl)porphynatemanganese(III) centers. An unusual pseudozero-order mechanism was observed by monitoring the formation of the cyclohexanol and cyclohexanone products, and a consistent oxygen-transfer mechanism, activated by the manganese center, was proposed on the light of the kinetic behavior. The k_H/k_D values suggested that in Mn(3-TRPyP) catalysis, the kinetics are favored by the stereochemical environment provided by the out-of-plane ruthenium complexes, whereas for the coplanar Mn(4-TRPyP) catalyst, the favorable electronic interaction of the ruthenium complexes with the metalloporphyrin center is the most relevant factor enhancing reactivity.

Keywords: Supramolecular catalysis; Tetraruthenated metalloporphyrins; Zero-order kinetics; Cyclohexane oxidation

1. Introduction

Metalloporphyrins have received special attention because of their catalytic, electrocatalytic, and electron-transfer properties [1–8], which are directly related to the stabilization of the transition metal ion in high oxidation states by the formation of M^{IV}=O– and M^{V}=O–like species [9–13]. By exploiting the coordination chemistry strategy for self-assembling supramolecular systems [2,14], transition metal complexes can be connected to the periphery of pyridylporphyrins [15,16] to modify the stereochemical environment or even to modulate the electronic characteristics of the metalloporphyrin center. As a matter of fact, supramolecular porphyrins containing selected peripheral metal complexes have been designed as biomimetic models of cytochrome P-450 [17,18]. As typical substituents, one can exploit the electron donor/acceptor and/or electron-transfer properties of the ancillary complexes or make use of them as cofactors, creating new pathways for the oxidation of organic substrate [19–21].

In this work we report a kinetic/mechanistic investigation of the oxidation reaction of cyclohexane by PhIO, catalyzed by tetraruthenated manganese(III) porphyrin species in two isomeric forms. Such catalysts were obtained by the coordination of four $[Ru(bpy)_2Cl]^+$ complexes to the pyridyl groups of *meso*-tetra(3-pyridyl)porphynatemanganese(III) [Mn(3-TRPyP)] and *meso*-tetra(4-pyridyl)porphynatemanganese(III) [Mn(4-TRPyP)], as shown in Fig. 1.

2. Experimental

2.1. Materials

The dichloromethane solvent was distilled over P_2O_5, and HPLC-grade acetonitrile was used as supplied. Both solvents were stored on 3 Å molecular sieves. *n*-Octane, used as an internal standard, was distilled, and its purity was confirmed by gas chromatography. All other chemicals were reagent grade (1,2-dichloroethane, cyclohexane, methanol, and deuterated cyclo-

* Corresponding author.
E-mail address: koiaraki@iq.usp.br (K. Araki).

0021-9517/$ – see front matter
doi:10.1016/j.jcat.2005.09.003

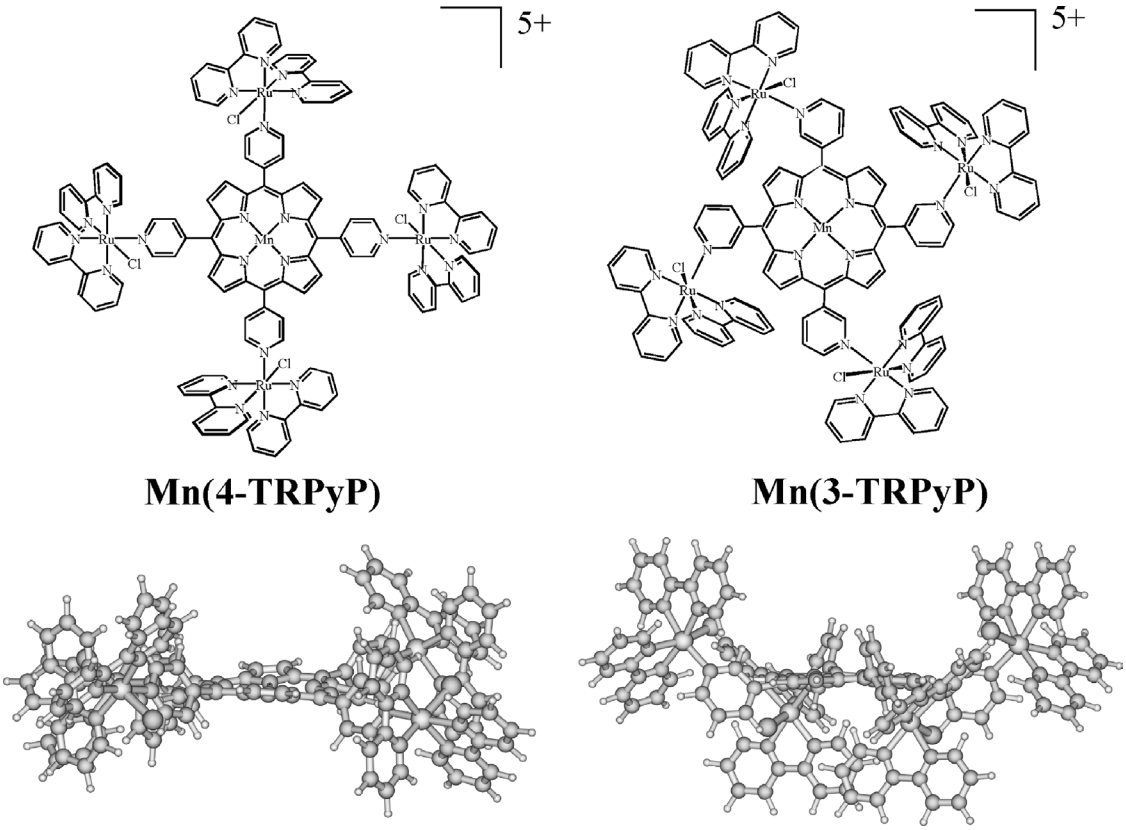

Fig. 1. Schematic and optimized DFT structures of the two manganese(III) porphyrin isomers, Mn(3-TRPyP) and Mn(4-TRPyP).

hexane with > 99% D) and used as received. Iodosylbenzene (PhIO) was prepared from iodobenzene diacetate and NaOH [22,23], and its purity (> 98%) was confirmed by the iodometric method. The supramolecular porphyrins were obtained and characterized previously [2,3].

2.2. Kinetics measurements

All reactions were carried out under a nitrogen atmosphere, in a 25.0 ± 0.1 °C thermostatted 2 mL vial, capped with a Teflon-coated septum and containing a small magnetic stirring bar. Iodosylbenzene (1.1×10^{-5} mol), 1,2-dichloroethane (DCE; 130 µL), cyclohexane (200 µL), and *n*-octane (1 µL of a *n*-octane/DCE, 5.9 mg/75 mg solution) were successively transferred with a Hamilton syringe, and, finally, a precise volume of the catalyst stock solution in acetonitrile (ACN) was added. To vary the concentration of the catalyst while keeping the experimental conditions constant, a complementary volume of ACN was added to the reacting mixture. Then gas chromatography (GC) analyses were performed with a Shimadzu GC-17A device, using a flame ionization detector and a 30 m × 0.25 mm OV-1701, 0.25-µm capillary column. Nitrogen was used as carrier gas.

2.3. UV–vis spectroscopy

Spectral changes after addition of a iodosylbenzene CH_2Cl_2:CH_3OH:H_2O (80:18:2) solution, into 2 mL of 4.6×10^{-6} mol dm^{-3} solution of Mn(3-TRPyP) or Mn(4-TRPyP) in acetonitrile (cat:PhIO = 1:26 and 1:52, respectively), were recorded on an HP-8453 diode-array spectrophotometer.

3. Results and discussion

3.1. Electronic spectroscopy

A shift of the so-called porphyrin band V (Fig. 2), from 473 to 428 nm was observed in the electronic absorption spectra after addition of PhIO, concomitantly with the disappearance of bands III and IV and the decrease of bands V_a and VI. The Mn(III)P is consumed in few seconds and the oxidized O=Mn^{IV}(TRPyP) species accumulates allowing its UV–vis spectroscopic detection in solution. In all experiments, the bands associated with the peripheral ruthenium complexes ($p\pi \rightarrow p\pi^*$, $MLCT_2$ and $MLCT_1$ at 295, 350, and 495 nm) did not change significantly. Such observations are consistent with the formation of the O=Mn^{IV}P species from oxidation of the starting Mn(3-TRPyP) and Mn(4-TRPyP), while keeping the peripheral complexes unchanged. This is an interesting aspect, because the redox potential of these peripheral complexes was found to be lower than for the oxidation of the Mn(III)P center by cyclic voltammetry, clearly demonstrating the fundamental role of the oxygen-transfer process in the activation of the metalloporphyrin site. However, it should be noticed that the O=Mn^{IV}P species may not be the primarily formed species. In general, as previously reported for similar manganese por-

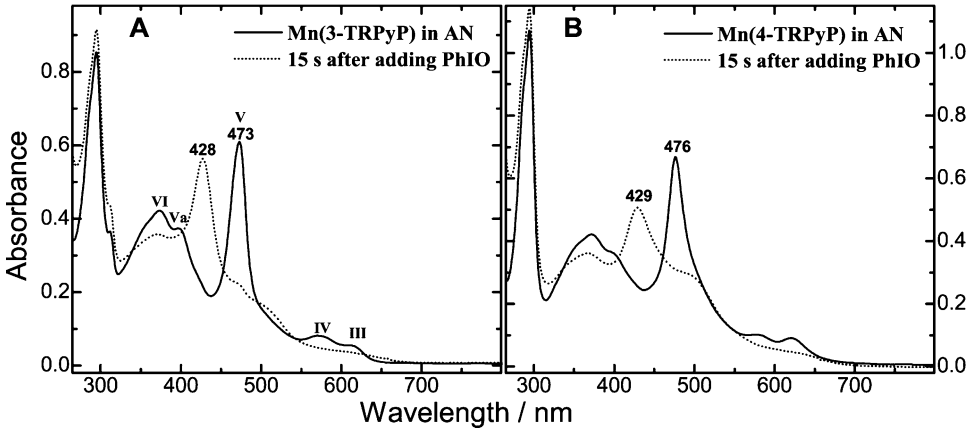

Fig. 2. UV–vis spectra obtained before and 15 s after addition of 2.36×10^{-2} mol dm^{-3} iodosylbenzene CH_2Cl_2:CH_3OH:H_2O (80:18:2) solution, into an acetonitrile solution of (A) Mn(3-TRPyP) and (B) Mn(4TRPyP). [MnP] = 4.6×10^{-6} mol dm^{-3}; [cat]:[PhIO] = 1:10.

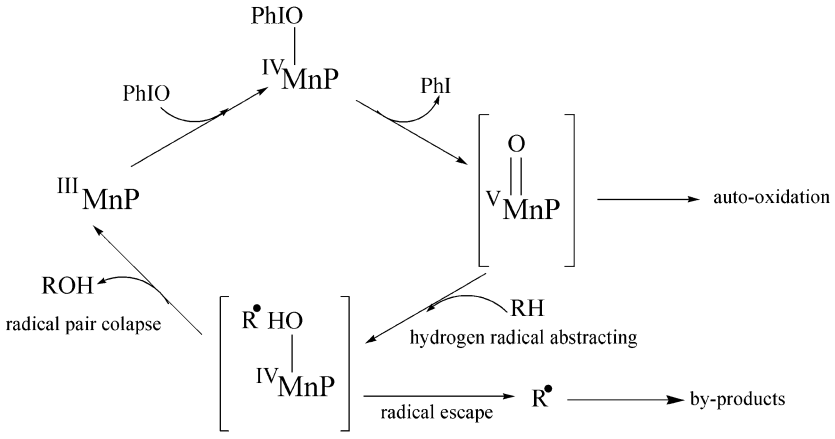

Scheme 1. Hydroxylation mechanism of cyclohexane catalyzed by Mn porphyrins.

phyrins [9,13], it is considered just a stable high-valent species, generated after the fast decay of the real catalytic active species, O=Mn^{V}P.

3.2. Determination of kinetic parameters

The oxidation of cyclohexane with PhIO in the presence of the supramolecular Mn(3-TRPyP) and Mn(4-TRPyP) species, at 25 °C, was found to yield cyclohexanol and cyclohexanone as major products

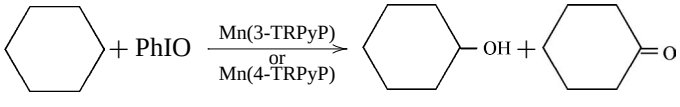

(1)

None of these products could be found in the absence of those manganese species, showing that they are in fact mediating the oxygen atom transfer to that substrate.

It is interesting to notice that a small but significant amount of chlorocyclohexane was also detected as a byproduct of the reaction. This species was not detected when the conventional porphyrins, MnTPyP or MnTMPyP, were used as catalyst. The abstraction of chloro atoms from the solvent DCE is improbable, because it was not observed when a related highly active catalyst, MnTCP, was used [19]. Accordingly, the evidence supports the conclusion that the chloride atom is being abstrated from the peripheral complexes in the supramolecular catalyst, which suggests a mechanism similar to the oxygen-atom rebound proposed by Groves [24,25] for metalloporphyrins (Scheme 1). In this mechanism, the active oxo-species cleaves the C–H bond abstracting a hydrogen atom and the cyclohexyl radical subsequently reacts with the bond OH group, yielding cyclohexanol, as shown in Scheme 1. According with this model, cyclohexanone is formed by further oxidation of cyclohexanol. However, the cyclohexyl radical may eventually escape from the cage reacting with the chloride ligand in the peripheral ruthenium complexes or abstracting a chlorine atom from DCE solvent, as proposed previously [6,21].

To elucidate the mechanism, the concentrations of the products were monitored as a function of the time by GC, using 1-μL samples. Typical kinetic plots are shown in Fig. 3. It should be noted that the concentration of all products increased linearly as a function of the reaction time for at least two half-lives. There is a short induction period of about 15 s, including the mixing time. The kinetics is consistent with a zero-order mechanism relative to the formation of the products [26], that is, the reaction rate is apparently independent of the concentration of the reactants, as expressed by Eq. (2) [27]. The total concentra-

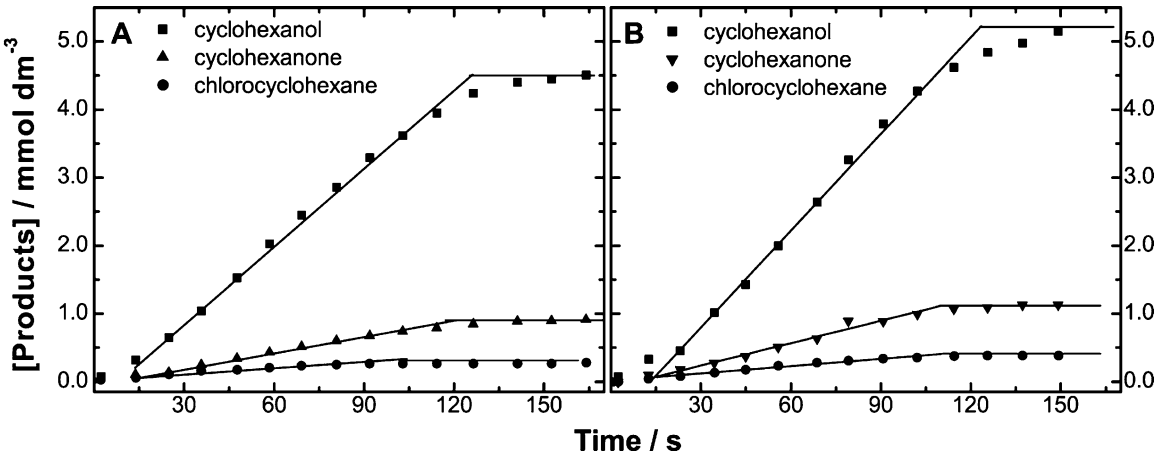

Fig. 3. Variation of the reaction products concentration as a function of the time after addition of (A) Mn(3-TRPyP) and (B) Mn(4-TRPyP) ACN solution into a mixture of cyclohexane and PhIO in 130 μL of DCE. The volume of ACN in the reaction mixture was kept constant at 50 μL. Conditions: [MnP] = 2.96×10^{-4} mol dm^{-3}; [PhIO] = 0.3 mol dm^{-3} (considering that it is in solution); [cyclohexane] = 4.8 mol dm^{-3} (200 μL); total volume = 381 μL; $T = 25\,^{\circ}$C; under a nitrogen atmosphere.

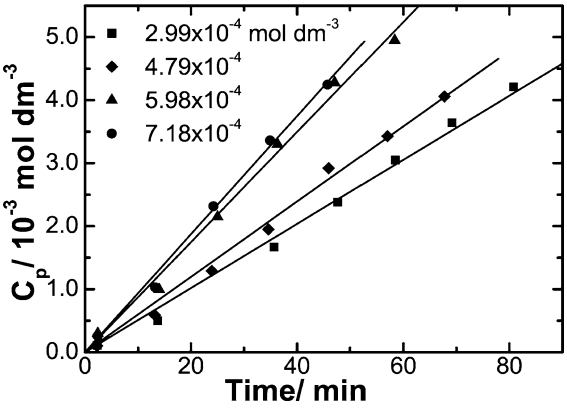

Fig. 4. Change of the products concentration *vs.* time for the cyclohexane oxidation with PhIO, catalyzed by different concentrations of Mn(3-TRPyP). Conditions: PhIO = 0.03 mol dm^{-3}; cyclohexane = 4.8 mol dm^{-3} (200 μL); total volume = 381 μL; $T = 25\,^{\circ}$C; under nitrogen atmosphere.

tion of the reaction products also varied according to a linear function of the reaction time. However, the zero-order rate constants (k_{obs}; Fig. 4) showed a linear dependence with respect to the catalyst concentration (Fig. 5). Furthermore, the zero-order kinetic behavior is only broken down when the reaction approaches the endpoint, when the PhIO reagent is depleted. This behavior can be satisfactorily explained considering the following points:

1. PhIO is only slightly soluble in the medium; its concentration should remain approximately constant inasmuch as the solid reagent is present in the reaction mixture.
2. There is a very large excess of cyclohexane (the [catalyst]/[cyclohexane] ratio is typically 1:16,000) and its concentration can be considered constant.
3. The concentration of the catalytic active species formed in solution depends on the initial concentration of its precursor [Mn(3-TRPyP) and Mn(4-TRPyP)], remaining constant during the kinetics.

In this way,

$$\frac{dC}{dt} = k. \tag{2}$$

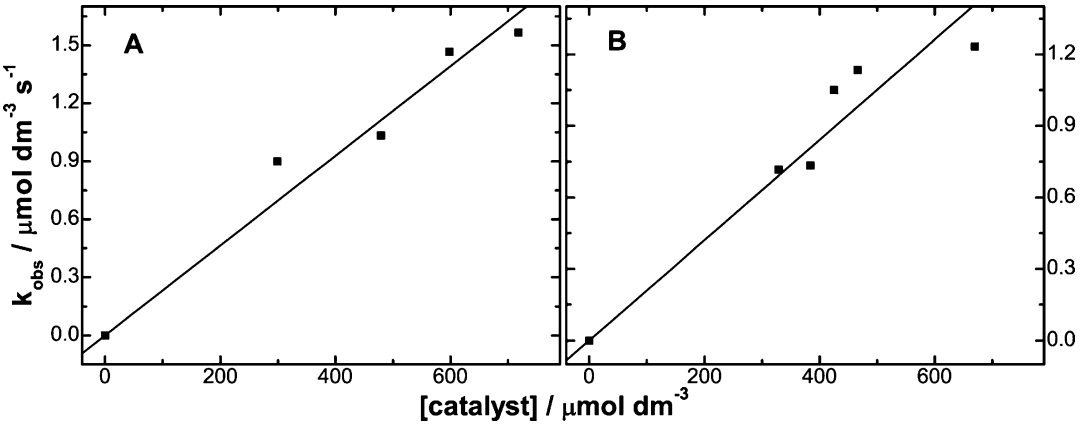

Fig. 5. Plot of the zero-order rate constants (k_{obs}) as a function of (A) Mn(3-TRPyP) and (B) Mn(4-TRPyP) concentration. Conditions: PhIO = 0.03 mol dm^{-3}; cyclohexane = 4.8 mol dm^{-3} (200 μL); total volume = 381 μL; $T = 25\,^{\circ}$C; under nitrogen atmosphere.

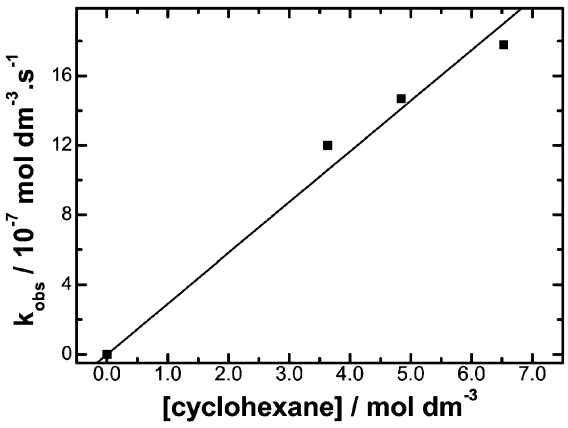

Fig. 6. Change at the experimental rate constant (k_{obs}) with the concentration of cyclohexane. Conditions: [Mn(3-TRPyP)] = 5.98×10^{-4} mol dm^{-3}; PhIO = 0.03 mol dm^{-3}; cyclohexane = 4.8 mol dm^{-3} (200 μL); total volume = 381 μL; $T = 25\,^{\circ}$C; under nitrogen atmosphere.

Accordingly, the rate constants independent of the catalyst concentration (k'_{obs}) can be determined from the angular coefficients of the curves shown in Fig. 5. However, when experiments varying the concentration of the substrate were carried out, a linear dependence between k_{obs} and [cyclohexane] was also evidenced using Mn(3-TRPyP) (Fig. 6) and Mn(4-TRPyP) as catalyst. Consequently, the catalytic reaction also exhibits a first-order dependence in relation to [cyclohexane]. This result is in agreement with our previous assumption because cyclohexane is in large excess assuring a pseudofirst-order condition relative to the substrate. Considering the dependence of the catalyst and substrate concentration, the second-order rate constant for the reaction $k_{cat} = k_{obs}/([\text{catalyst}][\text{cyclohexane}])$ equal to $(4.7 \pm 0.2) \times 10^{-4}$ M^{-2} s^{-1} and $(4.3 \pm 0.2) \times 10^{-4}$ M^{-2} s^{-1} were obtained, respectively, for Mn(3-TRPyP) and Mn(4-TRPyP).

Diffuse Fourier transform calculations had been used to explain the electronic coupling observed between the porphyrin ring and the peripheral *meso*-phenyl groups [28,29]. Accordingly, electronegative substituents on the phenyl ring tend to contribute to the porphyrin ring stabilization against oxidation, by diminishing the electronic density on it [30,31]. Similar effects are expected for the supramolecular *meso*-pyridylporphyrins. In fact the optimized geometry of Mn(3-TRPyP) and Mn(4-TRPyP) species, obtained by DFT and molecular mechanics calculations [32–34] showed that the macrocyclic ring is essentially planar. Furthermore, the peripheral ruthenium ions are in the same plane in the Mn(4-TRPyP) species, but they are located above and below the porphyrin plane in the case of Mn(3-TRPyP) complex (Fig. 1).

The catalytic activity can be modulated by the electronic effects induced by the peripheral ruthenium complexes. In contrast, the stereochemical positioning of these groups with respect to the porphyrin center can also give rise to local picket fences, or pockets, influencing the accommodation of the substrates near the catalytic site. The first contribution should be more effective in the case of Mn(4-TRPyP) than the Mn(3-TRPyP) isomer because of the nodal plane found in the pyridyl bridge for the last species, inhibiting the electronic coupling.

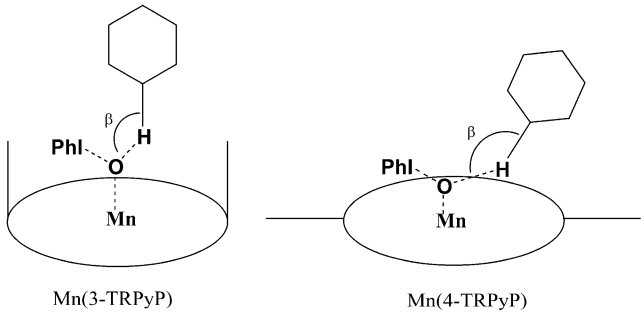

Fig. 7. Schematic transition state geometry in the cyclohexane hydroxylation with PhIO, catalyzed by Mn(3-TRPyP) and Mn(4-TRPyP).

The second effect should be particularly important in the Mn(3-TRPyP) isomer, considering its particular geometry that generates two pockets above and below the porphyrin ring. The fact that Mn(3-TRPyP) isomer is slightly more active than the Mn(4-TRPyP) species, reflects the importance of the stereochemical effects in such supramolecular catalysts.

3.3. Kinetic isotopic effect (KIE)

The kinetic studies described earlier showed that the zero-order behavior is actually determined by the experimental conditions used. To shed some light on the structure of the activated complex, kinetic isotopic effects were investigated using deuterated cyclohexane (C_6D_{12}). According to Meunier [35,36], a very low KIE ($k_H/k_D < 1.8$) is associated with a transition state in which the iodobenzene-leaving group is still present, decreasing the β angle as shown in Fig. 7. As this angle approaches 90°, the KIE tends to 1, because the contribution of the asymmetric vibrations involved in the rate-determining step is oriented in orthogonal directions. Interestingly, no KIE was observed for Mn(3-TRPyP) ($k_H/k_D = 0.94 \pm 0.07$), whereas a small but significant effect was found in the case of the Mn(4-TRPyP) isomer (1.7 ± 0.3). Accordingly, as expected, the stereochemical environment provided by the peripheral ruthenium complexes in the Mn(3-TRPyP) species should be favoring the formation of an activated complex in which the β angle is smallest as possible. This is also corroborated by the slightly higher reaction rate found for the Mn(3-TRPyP) isomer. Because of its planar geometry, such effect should be relatively less important in the Mn(4-TRPyP) *para*-isomer, leading to a more relaxed transition state, as illustrated in Fig. 7.

3.4. Reaction mechanism

Based on the results described herein, the mechanism shown in Scheme 2 can be proposed. The first step involves the rapid reaction between the manganese(III) porphyrin precursor with iodosylbenzene yielding an adduct, namely AB. This intermediate associates with cyclohexane forming the active key intermediate ABD, in which the KIE takes place. Next, the C–H cleavage proceeds generating in the same cage trapped cyclohexyl radical and OH groups that recombine rapidly, yielding cyclohexanol and regenerating the starting Mn(II)P. This product can be oxidized once again forming cyclohexanone.

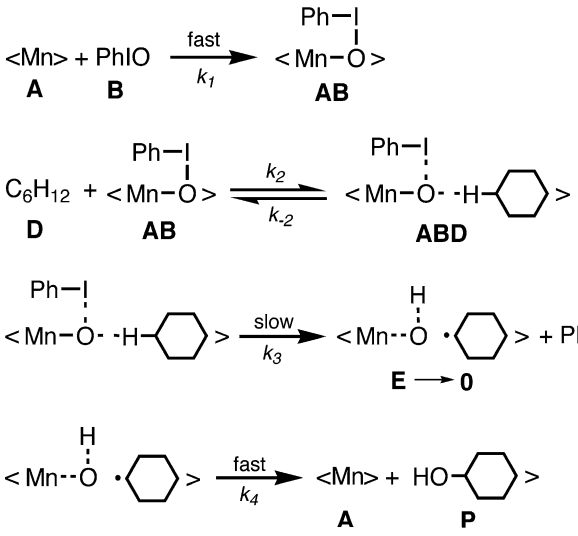

$$\frac{d[AB]}{dt} = k_1[A][B] \quad (3)$$

$$\frac{d[ABD]}{dt} = k_2[D][AB] - k_{-2}[ABD] - k_3[ABD] \quad (4)$$

$$\frac{d[E]}{dt} = k_3[ABD] - k_4[E] \quad (5)$$

$$\frac{d[P]}{dt} = k_4[E] \quad (6)$$

Scheme 2. Scheme showing the elementary reactions and the corresponding differential rate equations for the mechanism proposed for the Mn(3-TRPyP) and Mn(4-TRPyP) catalyzed cyclohexane oxidation by PhIO.

Considering the hypothesis of stationary state for ABD and E,

$$k_2[D][AB] - (k_{-2} + k_3)[ABD] = 0, \quad (7)$$

$$[ABD] = k_2[D][AB]/(k_{-2} + k_3), \quad (8)$$

and

$$k_3[ABD] - k_4[E] = 0. \quad (9)$$

Accordingly,

$$\frac{d[P]}{dt} = k_3[ABD]. \quad (10)$$

Substituting Eq. (8) in (10), and considering that [AB] is proportional to [A],

$$\frac{d[P]}{dt} = \frac{k_3 k_2[AB][D]}{k_3 + k_{-2}}, \quad (11)$$

$$\frac{d[P]}{dt} = k_{cat}[A][D]. \quad (12)$$

Hence the rate equation for cyclohexane oxidation by PhIO catalyzed by Mn(3-TRPyP) and Mn(4-TRPyP) complexes is given by Eq. (12). This is consistent with our experimental results and explains the observed pseudozero-order kinetic behavior, because the concentration of cyclohexane is in large excess ([D] ≈ constant) and for a single run, the concentration of catalyst is also constant ([A] ≈ constant) if no decomposition takes place.

It should be noted that cyclohexyl radical can eventually escape from the local cage and abstract chlorine atoms from the neighborhood, forming the observed chlorinated byproduct. In our case, the peripheral $[Ru(bpy)_2Cl]^+$ groups provide a readily accessible source of chlorine atoms, particularly in the Mn(3-TRPyP) case. This conclusion is supported by preliminary experiments, carried out under similar conditions, with manganese(III) porphyrins containing peripheral $[Ru_3O(Ac)_6(py)_2]^{3+}$ groups (Mn-TCP), instead of $[Ru(bpy)_2Cl]^+$. In this case, the solvent is the only source of chlorine atoms, but no evidence of chlorinated byproducts have been found.

4. Conclusions

The supramolecular manganese porphyrin Mn(3- and 4-TRPyP) catalyzes the oxidation reaction of cyclohexane by iodosylbenzene, according to zero-order kinetics, expressed in terms of the concentration of the products as a function of time. The observed rate constants exhibited a first-order dependence on the catalyst and substrate concentrations. Small kinetic isotopic effects were observed for the catalytic process, being negligible for the Mn(3-TRPyP) isomer, and significant in the case of Mn(4-TRPyP), reflecting the stereochemical differences around the catalytic active site. The kinetics were consistent with an oxygen-transfer mechanism, in which the activated complex exhibits distinct contribution from the supramolecular electronic and stereochemical effects induced by the ancillary ruthenium complexes in the two isomers.

Acknowledgments

Financial support from FAPESP (Fundação de Amparo à Pesquisa do Estado de São Paulo), CNPq (Conselho Nacional de Desenvolvimento Científico e Tecnológico), CAPES/PICD, RENAMI (Rede de Nanomateriais Moleculares e de Interface), and the Millenium Institute of Complex Materials is gratefully acknowledged.

References

[1] B. Meunier, Chem. Rev. 92 (1992) 1411.
[2] H.E. Toma, K. Araki, Coord. Chem. Rev. 196 (2000) 307.
[3] K. Araki, H. Winnischofer, H.E.B. Viana, M.M. Toyama, F.M. Engelmann, I. Mayer, A.L.B. Formiga, H.E. Toma, J. Electroanal. Chem. 562 (2004) 145.
[4] K. Araki, L. Angnes, H.E. Toma, Adv. Mater. 7 (1995) 554.
[5] J.R.C. da Rocha, G.J.F. Demets, M. Bertotti, K. Araki, H.E. Toma, J. Electroanal. Chem. 526 (2002) 69.

[6] M.J. Nappa, R.J. McKinney, Inorg. Chem. 27 (1988) 3740.
[7] Z.W. Tong, T. Shichi, K. Takagi, Mater. Lett. 57 (2003) 2258.
[8] T.C. Zheng, D.E. Richardson, Tetrahedron Lett. 36 (1995) 833–836.
[9] J.T. Groves, J. Lee, S.S. Marla, J. Am. Chem. Soc. 119 (1997) 6269.
[10] T.J. Groves, M.K. Stern, J. Am. Chem. Soc. 110 (1988) 8628.
[11] N. Jin, J.T. Groves, J. Am. Chem. Soc. 121 (1999) 2923.
[12] A. Yamamoto, L.K. Phyllips, M. Calvin, Inorg. Chem. 7 (1968) 847.
[13] J.A. Smegal, C.L. Hill, J. Am. Chem. Soc. 105 (1983) 2920.
[14] C.M. Drain, C. Kirmaier, C.J. Medfoth, D.J. Nurco, K.M. Smith, D. Holten, J. Phys. Chem. 100 (1996) 11986.
[15] A. Osuka, T. Nagata, K. Maruyama, Chem. Lett. (1991) 1687.
[16] R.D. Hartnell, D.P. Arnold, Organometallics 23 (2004) 391.
[17] D.R. Benson, R. Valentekovich, F. Diederich, Angew. Chem. Int. Ed. Engl. 29 (1990) 191.
[18] C.C. Guo, Acta Chim. Sinica 52 (1994) 367.
[19] S. Dovidauskas, H.E. Toma, K. Araki, H.C. Sacco, Y. Iamamoto, Inorg. Chim. Acta 305 (2000) 206.
[20] C.-C. Guo, H.-P. Li, J.-B. Xu, J. Catal. 185 (1999) 345.
[21] C.-C. Guo, J.-X. Song, X.-B. Chen, G.-F. Jiang, J. Mol. Catal. A 157 (2000) 31.
[22] H.J. Lucas, E.R. Kennedy, M.W. Formo, Org. Synth. Coll. 3 (1955) 483.
[23] J.G. Sharefkin, H. Saltzmann, Org. Synth. 43 (1963) 62.
[24] J.T. Groves, D.V. Subramanian, J. Am. Chem. Soc. 106 (1984) 2177.
[25] J.T. Groves, J. Chem. Educ. 62 (1985) 928.
[26] C.C. Guo, J. Catal. 178 (1998) 182.
[27] K.A. Connors, Chemical Kinetics: The Study of Reaction Rates in Solution, VCH Publishers, New York, 1990.
[28] A. Rosa, G. Ricciardi, E.J. Baerends, A. Romeo, L.M. Scolaro, J. Phys. Chem. A 107 (2003) 11468.
[29] V.S. Chirvony, A.v. Hoek, V.A. Galievsky, I.V. Sazanovich, T.J. Schaafsma, D. Holten, J. Phys. Chem. B 104 (2000) 9909.
[30] R.F. Parton, I.F.J. Vankelecom, D. Tas, K.B.M. Janssen, P.P. Knops-Genits, P.A. Jacobs, J. Mol. Catal. A 125 (1996) 283.
[31] D. Mansuy, Coord. Chem. Rev. 125 (1993) 129.
[32] I. Mayer, A.L.B. Formiga, F.M. Engelmann, H. Winnischofer, P.V. Oliveira, D.M. Tomazela, M.N. Eberlin, H.E. Toma, K. Araki, Inorg. Chim. Acta 358 (2005) 2629.
[33] I. Mayer, M.N. Eberlin, D.M. Tomazela, H.E. Toma, K. Araki, J. Brazil Chem. Soc. 16 (2005) 418.
[34] D.M. Tomazela, F.C. Gozzo, I. Mayer, F.M. Engelmann, K. Araki, H.E. Toma, M.N. Eberlin, J. Mass. Spectrom. 39 (2004) 1161.
[35] P. Hoffmann, A. Robert, B. Meunier, Bull. Soc. Chim. Fr. 129 (1992) 85.
[36] A. Sorokin, A. Robert, B. Meunier, J. Am. Chem. Soc. 115 (1993) 7293.